2011 International Conference on Information and Electronics Engineering
IPCSIT vol.6 (2011) © (2011) IACSIT Press, Singapore

A Study for an Adaptive Anti-Jamming Antenna for the User Receiver of the GEO Satellite Communication System

Luis Germán Aponte Reyes[1], Shen Shi Tuan and Tan Zhan Zhong

School of Electronic and Information Engineering, Beijing University of Aeronautics and Astronautics, Beijing 100191, China

Abstract. The separation angle between geostationary earth orbit (GEO) satellites tends to be smaller owing to the increasing demand of high-speed fixed satellite services. This will increase the interferences from adjacent satellites at the user receivers of the GEO satellite communication systems. The commonly very small aperture terminal (VSAT) used by user receivers of these systems has no capability to cancel jammers. The objective of this document is to present the study of an adaptive anti-jamming antenna to replace the traditional VSAT at the user receiver and improve the anti-jamming performance of a real GEO satellite communication system. In this study, we considered the characteristics of a fixed satellite service (FSS) and a GEO satellite communication system to design a square array (SA) of antennas that could replace the VSAT and meet the requirements of the system. The SA was divided into square sub-arrays (SSAs) and the linear constraint minimum variance (LCMV) algorithm was used to control the outputs of these SSAs to introduce a small gain in the directions of arrival (DOAs) of the jammers and guarantee the required gain in the direction of arrival (DOA) of the useful signal. We designed a simulation system to verify the performance of the adaptive anti-jamming antenna. In the simulations, we introduced two jammers at the user receiver from different DOAs. We simulated the performance of the uncontrolled antenna, and the degradation of the signal-to-jammer-plus-noise ratio (SJNR) due to the jammers was verified. After the antenna was controlled (by LCMV), the SJNR was improved and met the requirement. The results demonstrate that the adaptive anti-jamming antenna can replace the VSAT to fulfill the system requirements and cancel possible interferences.

Keywords: Anti-jamming, Communication Satellite, Antennas Array, VSAT, LCMV.

1. Introduction

The International Telecommunication Union (ITU) has established recommendations and regulations to avoid interferences at the user receivers of GEO-FSS [5]. Most of these recommendations have been developed for *2°* or *3°* satellite spacing in GEO. However, the increasing demand of commercial high-speed services is promoting the creation of new GEO communications satellite systems [6], which suggests that the minimum separation angle between satellites tends to be smaller. With this reduction of the separation angle, the coordination could be ineffective and the adjacent satellite interferences could become a serious problem. On the other hand, multiples evidences show that the commercial GEO satellite communications has been intentionally jammed [4].

The commercial VSAT, commonly used by user receivers of GEO-FSS, has no anti-jamming capability.

One of the most popular techniques to mitigate jamming is the adaptive anti-jamming antenna, but normally it is not used in commercial GEO satellite communication systems.

Under this background, this study proposes an adaptive anti-jamming antenna that can replace the VSAT to improve the anti-jamming capability of a real GEO satellite communication system.

Our approach is based on a ka band GEO-FSS (*28GHz* uplink and *19GHz* downlink) to create an interference environment at the VSAT of the user receiver. The downlink power flux density (FD_{dw}) at the user receiver is *-120.1dBW/m*^{2}, the received power of the useful signal (P_u) is *-129.4dBW* by using a VSAT of diameter *50cm* and *60%* efficiency, the noise power at the user receiver (P_n) is *-138.1dBW* for a channel

[1] Corresponding author. Telf.: +86 13488642469
E-mail address: luis_aponte80@hotmail.com

bandwidth *7.65MHz* and the receiver system noise temperature *148.2K*. The signal-to-noise ratio (SNR) at the user receiver is *8.7dB*. We considered this SNR as the minimum requirement of the system, so it is also the SJNR. A jammer with power flux density equal to *-90dBW/m²*, concentrated in a direction (θ_j, ϕ_j) close to the DOA of the useful signal, reduces the SJNR from *8.7dB* to ≈ *-30.1dB*. This causes the interruption of the FSS.

We considered that the DOAs of jammers from adjacent satellites are known. The jammers reduce the output SJNR at the user receiver, so the VSAT becomes useless and it is replaced with an adaptive anti-jamming antenna. The adaptive anti-jamming antenna structure is a SA of isotropic elements. Here we assumed the element is isotropic for convenience and also because it does not lose the generality.

The SA needs many elements to achieve the same gain as the VSAT. In consequence, many elements make difficult the control of the antenna. So, we divided the SA into SSAs. Afterward, these SSAs are controlled by LCMV. The LCMV algorithm is used to mitigate the jammers (intentional or non-intentional) and to enhance the useful signal.

2. The Adaptive Anti-Jamming Antenna

The adaptive anti-jamming antenna is shown in Figure 1. The aperture of the SA has been calculated to introduce the same gain as the VSAT at the DOA of the useful signal. The SA is divided into *25* SSAs. Accordingly, the adaptive anti-jamming antenna is controlled by weights connected to the SSAs outputs. This control method reduces the number of weights to *25*, but simultaneously, it also reduces the degrees of freedom of the adaptive anti-jamming antenna. Nevertheless, we consider that *24* degrees of freedom allow the adaptive anti-jamming antenna to deal with the useful signal and enough number of jammers.

The LCMV can increase the gain at the DOA of the useful signal, and at the same time, decrease the gain at the DOAs of the jammers. However, LCMV must know the useful DOA and jammers DOAs in advance.

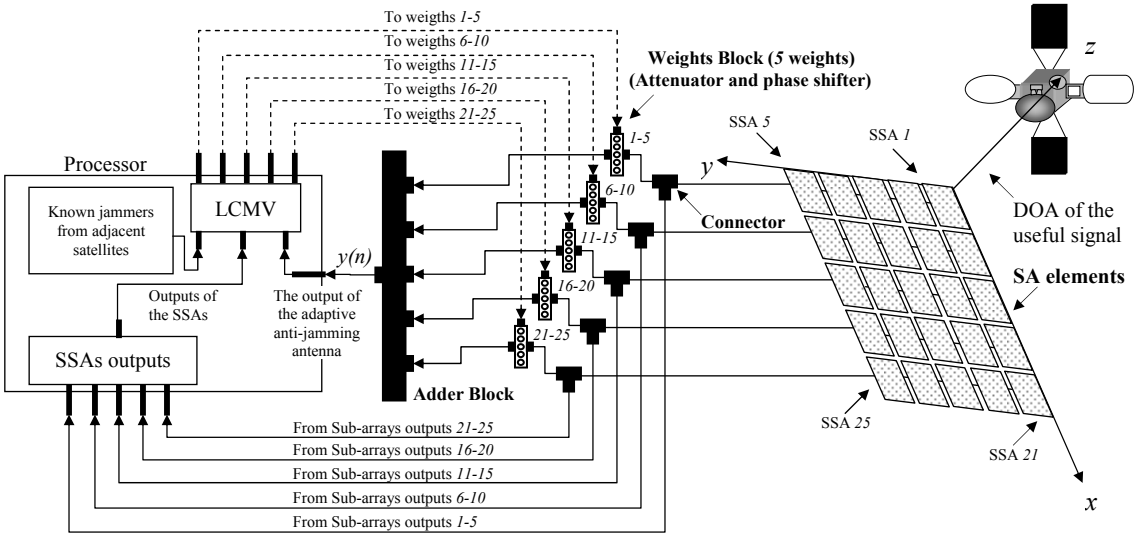

Fig. 1: Adaptive Anti-jamming Antenna to Replace the VSAT

In order to get the required gain of the system, the physical aperture of the SA must be ≥ $195.3\times10^{-3}\ m^2$. So, the number of isotropic elements in one dimension (*x* or *y*) of the SA must be >*3136*. We selected *3600* isotropic elements. This number of elements produces a directional radiation pattern with maximum power gain (at the DOA of the useful signal) of *38.3dBi* that satisfies SNR ≥ *8.7dB*.

The structure of the SA is depicted in Figure 2(a). It is an array of *5* by *5* elements, which are SSAs of *12* by *12* isotropic elements. The elements are equally spaced one-half wavelength ($\lambda/2$) apart, thus, the SSAs are spaced six-wavelength (6λ) apart. The effective aperture of de SSAs is $21.6\lambda^2$ ($53.85cm^2$) by assuming an efficiency of *60%*. The side length of the SA is 30λ (*47.37cm*) and the effective aperture is $540\ \lambda^2$ by assuming an efficiency of *60%*. The beamwidth of any SSA is *12.38°* and of the SA is *2.46°*. The output impedance, the polarization and the frequency bandwidth of the SA are assumed same as that of the VSAT.

A spherical coordinate system is used to represent the DOAs of the incoming signals (useful signal and jammers). The origin of the coordinate system is located at a corner of the SA; the z axis is oriented to the satellite. The incoming signals angles $\theta \in [0, 90^\circ]$ are measured from the z axis, and angles $\phi \in [0, 360^\circ]$ are measured from the x axis. The useful signal arrives from $\theta = 0^\circ$, thus, any ϕ can be considered. The jammers will arrive at the SA from DOAs (θ_j, ϕ_j).

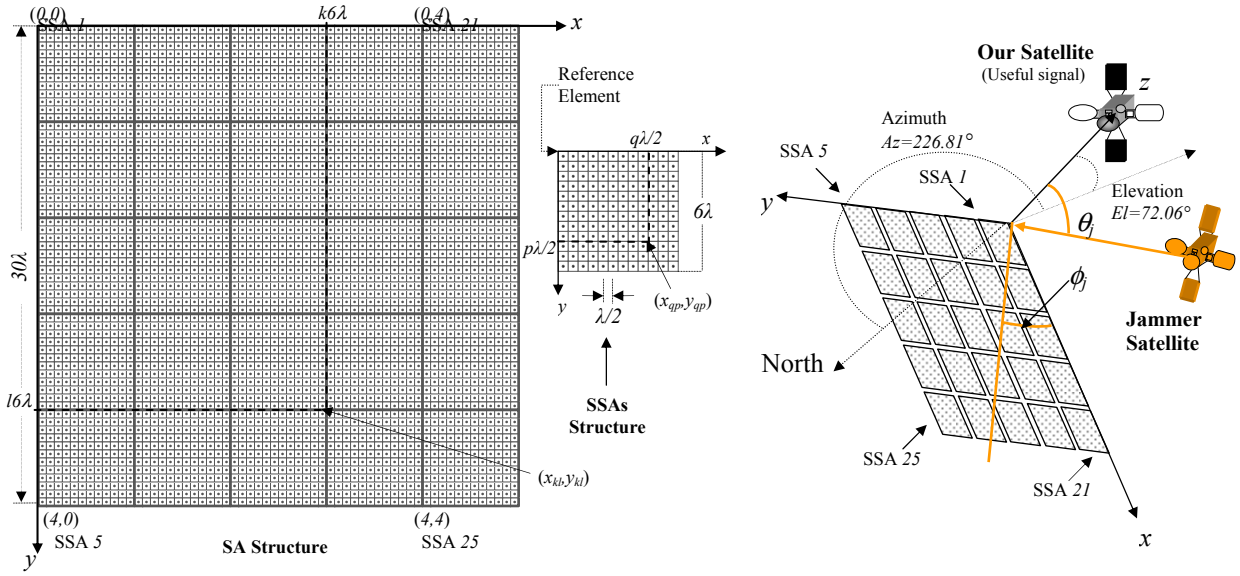

Fig. 2: (a) SA and SSAs Structure (Left). (b) SA Orientation (Right)

As shown in Figure 2, the reference element of a square sub-array (SSA) is located at the upper-left corner. In this element, the spatial phase of an incoming signal arriving from angle (θ,ϕ) is zero. The relative position of any other qp^{th} element (inside the same SSA) with respect to the reference, is given by $(x_{qp} = q\lambda/2, y_{qp} = p\,\lambda/2)$; so, the signal at this qp^{th} element is given by

$$y_{qp}(n) = s(n)e^{-j\pi[qSin\theta Cos\phi + pSin\theta Sin\phi]} = s(n)e^{j\zeta_{qp}} \quad 0 \le q \le 11;\ 0 \le p \le 11 \tag{1}$$

where $s(n)$ is a sample of the incoming signal from angle (θ,ϕ) measured at time n, and ζ_{qp} is the spatial phase at the qp^{th} element of the SSA.

From Eq.1, the output of the SSA is given by

$$x(n) = s(n)\sum_{q=0}^{11}\sum_{p=0}^{11} e^{j\zeta_{qp}} = s(n)f_{sub} \tag{2}$$

where f_{sub} is the field pattern of the SSA.

Note that the isotropic element is not a physical realizable type. However, for non-isotropic elements the output of the SSA can be computed by the principle of pattern multiplication [1]. Using this principle, we only need to multiply the field pattern of the non-isotropic element by Eq.2.

Considering that the position of a kl^{th} SSA (inside the *5* by *5* SA) is given by $(x_{kl} = k6\lambda, y_{kl} = l6\lambda)$, the signal at the output of that kl^{th} SSA is given by

$$x_{kl}(n) = s(n)f_{sub}e^{-j12\pi[kSin\theta Cos\phi + lSin\theta Sin\phi]} = s(n)f_{sub}e^{j\xi_{kl}} \quad 0 \le k \le 4;\ 0 \le l \le 4 \tag{3}$$

where $s(n)f_{sub}$ is given by Eq.2, and ξ_{kl} is a spatial phase due to the location of the kl^{th} SSA inside of the SA.

Let from Eq.3 to define two vectors $\boldsymbol{b}_x$ and $\boldsymbol{b}_y$ as in Eq.4 and Eq.5 respectively

$$\boldsymbol{b}_x(\theta,\phi) = [1 \quad e^{-j12\pi Sin\theta Cos\phi} \quad e^{-j24\pi Sin\theta Cos\phi} \quad e^{-j36\pi Sin\theta Cos\phi} \quad e^{-j48\pi Sin\theta Cos\phi}]^T \tag{4}$$

$$\boldsymbol{b}_y(\theta,\phi) = [1 \quad e^{-j12\pi Sin\theta Sin\phi} \quad e^{-j24\pi Sin\theta Sin\phi} \quad e^{-j36\pi Sin\theta Sin\phi} \quad e^{-j48\pi Sin\theta Sin\phi}]^T \tag{5}$$

The Kronecher product [2] of the two vectors $\boldsymbol{b}_x$ and $\boldsymbol{b}_y$, is given by

$$\boldsymbol{b}(\theta,\phi) = [\boldsymbol{b}_x(\theta,\phi) \otimes \boldsymbol{b}_y(\theta,\phi)] = [\boldsymbol{b}_1 \quad \boldsymbol{b}_2 \quad \boldsymbol{b}_3 \quad \boldsymbol{b}_4 \quad \boldsymbol{b}_5]^T \tag{6}$$

where $\boldsymbol{b}$ is a column vector of dimension 25×1. Each element of $\boldsymbol{b}$ is a row vector of dimension 1×5 given by

$$\boldsymbol{b}_{\varepsilon}=\begin{bmatrix} e^{-j(\varepsilon-1)12\pi Sin\theta Cos\phi} \\ e^{-j[(\varepsilon-1)12\pi Sin\theta Cos\phi+12\pi Sin\theta Sin\phi]} \\ e^{-j[(\varepsilon-1)12\pi Sin\theta Cos\phi+24\pi Sin\theta Sin\phi]} \\ e^{-j[(\varepsilon-1)12\pi Sin\theta Cos\phi+36\pi Sin\theta Sin\phi]} \\ e^{-j[(\varepsilon-1)12\pi Sin\theta Cos\phi+48\pi Sin\theta Sin\phi]} \end{bmatrix}^{T} \quad 1\le\varepsilon\le 5 \tag{7}$$

We can observe that each element of the column vector $\boldsymbol{b}$ corresponds with the spatial phase at each SSA output, and each spatial phase has two dimensions given by the angles (θ,ϕ). Therefore, the measured signals at the *25* SSAs outputs can be represented by

$$\boldsymbol{x}(n)=s(n)f_{sub}\boldsymbol{b}(\theta,\phi)=[x_1(n)\quad x_2(n)\quad .\ .\ .\ .\ .\ .\quad x_{25}(n)]^{T} \tag{8}$$

where $x_{\rho}(n)=s(n)f_{sub}e^{j\xi_{\rho}(\theta,\phi)}$ is the signal at the output of the ρ^{th} SSA ($1\le\rho\le 25$); $s(n)$ is a sample of the incoming signal from angle (θ,ϕ) measured at time n; f_{sub} is the field pattern of any SSA; and ξ_{ρ} is a spatial phase due to the location of the ρ^{th} SSA inside of the SA.

The weights connected to the *25* SSAs outputs are represented by

$$\boldsymbol{w}=[w_1\quad w_2\quad .\ .\ .\ .\ .\ .\quad w_{25}]^{T} \tag{9}$$

So, the output of the adaptive anti-jamming antenna $y(n)$ is given by,

$$y(n)=\boldsymbol{w}^{H}\boldsymbol{x}(n) \tag{10}$$

2.1. LCMV Algorithm

The objective of LCMV algorithm is to find a set of weights that will guarantee the adaptive anti-jamming antenna to introduce the required gain at the DOA of the useful signal and a small gain at the jammers DOAs. For this, the algorithm uses a linear constraint given by $\boldsymbol{C}^{H}\boldsymbol{w}_c=\boldsymbol{H}$. The matrix $\boldsymbol{C}$ is called "Constraint Matrix", $\boldsymbol{H}$ is the "Response Vector" and $\boldsymbol{w}_c$ is the weight vector obtained by the LCMV algorithm. In our system, the DOA of the useful signal and the DOAs of the jammers are well known. So, $\boldsymbol{C}$ is conformed by the steering vectors of the DOAs of incoming signals and $\boldsymbol{H}$ can be selected to introduce a required gain factor ($G_{required}$) at the DOA of the useful signal and a small gain factor (G_{small}) at the DOA of any jammer. Considering there are d incoming signals (useful + jammers), the steering vectors are given by,

$$\boldsymbol{a}_i=\boldsymbol{a}(\theta_i,\phi_i)=[a_{i1}\quad a_{i2}\quad \cdots\quad \cdots\quad a_{i25}]^{T}\qquad 1\le i\le d \tag{11}$$

where $a_{i\rho}=f_{sub}e^{j\xi_{\rho}(\theta_i,\phi_i)}$ ($1\le\rho\le 25$) . We selected $G_{required}=82.4$ and $G_{small}=1\times10^{-7}$ ($1\le j\le d-1$).

Using Lagrange Method and the Steepest Descend Method [3], the LCMV weight vector $\boldsymbol{w}_c$ is given by

$$\boldsymbol{w}_{c,m+1}=\psi[\boldsymbol{I}-\mu\boldsymbol{R}_{xx}]\boldsymbol{w}_{c,m}+\boldsymbol{w}_{qs}\rightarrow\psi=\boldsymbol{I}-\boldsymbol{C}(\boldsymbol{C}^{H}\boldsymbol{C})^{-1}\boldsymbol{C}^{H} \tag{12}$$

where the subscript m denotes the actual value at the m^{th} iteration, and $m+1$ denotes the updated value; $\boldsymbol{R}_{xx}=E[\boldsymbol{x}(n)\boldsymbol{x}^{H}(n)]$ is the autocorrelation matrix; E is the expected value; $\boldsymbol{w}_{qs}=\boldsymbol{C}(\boldsymbol{C}^{H}\boldsymbol{C})^{-1}\boldsymbol{H}$ is called the quiescent weight vector, which is the weight vector when there is no useful signal or jammers impinging on the adaptive anti-jamming antenna and only noise is considered, and $\mu=2/(\lambda_{\max}+\lambda_{\min})$ is a factor to control the convergence rate and the stability of the algorithm, where $\lambda_{\max}$ and $\lambda_{\min}$ are the maximum and minimum eigenvalues of the matrix $\psi\boldsymbol{R}_{xx}\psi$.

After LCMV, the power of the useful signal at the output of the antenna is $P_u(\theta_u,\phi_u)=\boldsymbol{w}_c^{H}\boldsymbol{a}_u\boldsymbol{a}_u^{H}\boldsymbol{w}_cP_{u,i}$; $P_{u,i}$ is the power of the useful signal at the input of the antenna; the power of a jammer at the output of the antenna $P_j(\theta_j,\phi_j)=\boldsymbol{w}_c^{H}\boldsymbol{a}_j\boldsymbol{a}_j^{H}\boldsymbol{w}_cP_{j,i}$; $P_{j,i}$ is the power of the jammer at the input of the antenna.

3. Simulations

3.1. Adaptive Anti-Jamming Antenna Simulation System (SS)

The block diagram of the adaptive anti-jamming antenna SS is shown in the following Figure 3. The EM is used to obtain the power flux density of the useful signal at the user receiver. The JNM works: 1) to simulate thermal noise at the output of the antenna as zero-mean Gaussian noise; 2) to introduce jammers (CW_j) and (WB_j) with different DOAs. The AARM is used: 1) to simulate the power pattern of the adaptive anti-jamming antenna when it is non-controlled; 2) to simulate the signal at the SSAs outputs; and 3) to

simulate the signal at the output of the antenna. LM is the LCMV algorithm module. It can be connected or not (ON-OFF) to the AARM by a virtual switch. If the switch is ON, LM controls the adaptive anti-jamming antenna by LCMV. The resulting weights will go to the AARM, and this module simulates the power pattern of the adaptive anti-jamming antenna when it is controlled. The PM receives the output from the AARM and estimates the output SJNR.

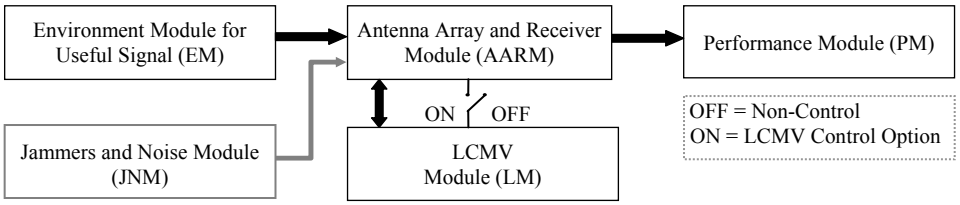

Fig. 3: Adaptive Anti-Jamming Antenna SS Blocks

3.2. Adaptive Anti-Jamming Antenna Simulation Process (SP)

In order to evaluate the performance of the adaptive anti-jamming antenna before and after being controlled by LCMV algorithms, six scenarios were defined as shown in Table 1.

Table 1. Scenarios for the SP

Scenario	CW_j [dBW/m^2]	θ	ϕ	WB_j [dBW/m^2]	θ	ϕ
1	*-90*	*1°*	*180°*	*-210*	*1°*	*0°*
2	*-90*	*1°*	*180°*	*-110*	*1°*	*0°*
3	*-90*	*1°*	*135°*	*-210*	*1°*	*315°*
4	*-90*	*1°*	*135°*	*-110*	*1°*	*315°*
5	*-90*	*1°*	*225°*	*-210*	*1°*	*45°*
6	*-90*	*1°*	*225°*	*-110*	*1°*	*45°*

For all the cases, it is assumed that the antenna is oriented to the satellite, so the DOA of the useful signal is (θ=*0*°, at any ϕ).

The first step in the SP is to check the performance of the adaptive anti-jamming antenna for the non-control option. The results in Table 2 show that it cannot meet the SJNR requirement.

Table 2. Adaptive Anti-Jamming Antenna for Non-Control Option

Scenario	P_u [*dBW*]	CW_j [*dBW*]	WB_j [*dBW*]	P_n [*dBW*]	SJNR [*dB*]
1	*-128.8*	*-103.1*	*-223.1*	*-138.1*	*-25.8*
2	*-128.8*	*-103.1*	*-123.1*	*-138.1*	*-25.8*
3	*-128.8*	*-102.8*	*-222.8*	*-138.1*	*-26.0*
4	*-128.8*	*-102.8*	*-122.8*	*-138.1*	*-26.1*
5	*-128.8*	*-102.8*	*-222.8*	*-138.1*	*-26.0*
6	*-128.8*	*-102.8*	*-122.8*	*-138.1*	*-26.1*

Subsequently, the antenna is controlled to improve the SJNR (switch ON). In SS, the LCMV option: 1) gets the steering vector for the DOA of the useful signal and the DOAs of the known jammers; 2) computes the constraint matrix $\boldsymbol{C}$ and the vector $\boldsymbol{H}$; and 3) calculates a weight vector ($\boldsymbol{w}_c$) by the iterative process described in Eq. 12.

With LCMV implementation, the matrix $\boldsymbol{C}$ and the vector $\boldsymbol{H}$ for the scenario 2 are given by

$$\boldsymbol{C}=[\boldsymbol{C}_1 \quad \boldsymbol{C}_2 \quad \boldsymbol{C}_3 \quad \boldsymbol{C}_4 \quad \boldsymbol{C}_5]^T \;;\; \boldsymbol{C}_1=\boldsymbol{C}_2=\boldsymbol{C}_3=\boldsymbol{C}_4=\boldsymbol{C}_5= 1.0e+2*\begin{bmatrix} 1.44 & 1.35-0.42i & 1.35+0.42i \\ 1.44 & 0.81-1.16i & 0.81+1.16i \\ 1.44 & -0.07-1.41i & -0.07+1.41i \\ 1.44 & -0.92-1.08i & -0.92+1.08i \\ 1.44 & -1.38-0.29i & -1.38+0.29i \end{bmatrix}^T \tag{13}$$

$$(\textit{for Scenario 2}) \quad \boldsymbol{H}=[\,8.24e+1 \quad 1.00e-7 \quad 1.00e-7\,]^T \tag{14}$$

From Eq.13 and Eq.14, the new weight vector $\boldsymbol{w}_c$ for LCMV is given by

$$(\textit{for Scenario 2}) \quad \boldsymbol{w}_c=[\boldsymbol{w}_1 \quad \boldsymbol{w}_2 \quad \boldsymbol{w}_3 \quad \boldsymbol{w}_4 \quad \boldsymbol{w}_5]^T \tag{15}$$

$$w_1 = \begin{bmatrix} 7.74e\text{-}2+3.23e\text{-}10i \\ -3.05e\text{-}3+1.40e\text{-}9i \\ -3.42e\text{-}2-4.06e\text{-}9i \\ -3.05e\text{-}3+4.66e\text{-}9i \\ 7.74e\text{-}2-1.47e\text{-}9i \end{bmatrix}^T \quad w_2 = \begin{bmatrix} 7.74e\text{-}2+1.98e\text{-}10i \\ -3.05e\text{-}3+1.08e\text{-}9i \\ -3.42e\text{-}2-4.10e\text{-}9i \\ -3.05e\text{-}3+4.10e\text{-}9i \\ 7.74e\text{-}2-1.60e\text{-}9i \end{bmatrix}^T \quad w_3 = \begin{bmatrix} 7.74e\text{-}2+8.69e\text{-}11i \\ -3.05e\text{-}3+1.05e\text{-}9i \\ -3.42e\text{-}2-3.99e\text{-}9i \\ -3.05e\text{-}3+4.14e\text{-}9i \\ 7.74e\text{-}2-1.69e\text{-}9i \end{bmatrix}^T \quad w_4 = \begin{bmatrix} 7.74e\text{-}2-1.46e\text{-}11i \\ -3.05e\text{-}3+1.47e\text{-}9i \\ -3.42e\text{-}2-3.94e\text{-}9i \\ -3.05e\text{-}3+4.36e\text{-}9i \\ 7.74e\text{-}2-1.93e\text{-}9i \end{bmatrix}^T \quad w_5 = \begin{bmatrix} 7.74e\text{-}2+1.29e\text{-}10i \\ -3.05e\text{-}3+1.30e\text{-}9i \\ -3.42e\text{-}2-4.37e\text{-}9i \\ -3.05e\text{-}3+4.40e\text{-}9i \\ 7.74e\text{-}2-1.89e\text{-}9i \end{bmatrix}^T$$

Figure 4 shows the power pattern of the adaptive anti-jamming antenna controlled by LCMV in the Scenario 2. We can observe that the adaptive anti-jamming antenna produces deep nulls of *-134dBi* and *-137.1dBi* at CW_j and BW_j DOAs respectively, and at the same time, produces constant gain of *38.3dBi* at the DOA of the useful signal. For all the scenarios, LCMV kept constant SJNR = *9.3dB*.

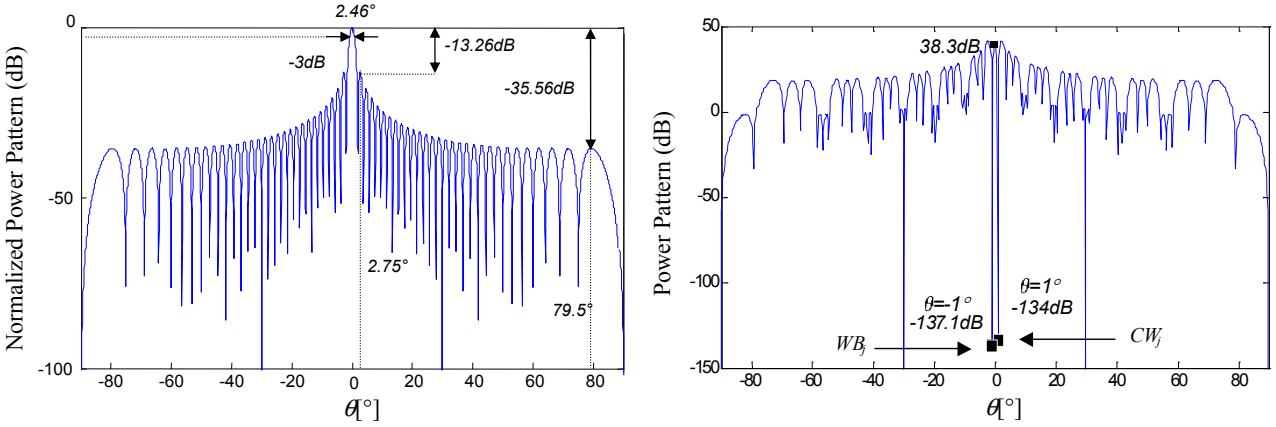

Fig. 4: Power Pattern of the Adaptive Anti-Jamming Antenna non-Controlled (left) and Controlled by LCMV in the Scenario 2 (right). Cut at $\phi=180°$

4. Conclusions

This study shows that it is possible to replace the VSAT of the user receiver with an adaptive anti-jamming antenna in the GEO satellite communication system. It was demonstrated that the adaptive anti-jamming antenna maintains the SNR ≥ *8.7dB* in a non-interference environment. Also, the antenna controlled by LCMV mitigates a CW_j = *-90dBW/m²* ($\theta = 1°$, at any ϕ) and a WB_j = *-110dBW/m²* ($\theta = 1°$, at any ϕ). In all the simulated scenarios, the constraint introduced by LCMV kept constant SJNR = *9.3dB*. LCMV introduced gain of *38.3dBi* at the DOA of the useful signal and gains < *-129 dBi* at the DOAs of the jammers. The adaptive anti-jamming antenna fulfill the system's gain requirements, it is easy to control and has the capability to cancel jammers at an angle of *1°* with respect to the DOA of the useful signal.

5. References

[1] John C. Kraus, Ronald J. Marhefka. *Antennas: For All Applications*, 3rd. ed. Beijing: McGraw-Hill Co. and Publishing House of Electronics Industry. 2008.

[2] Michael D. Zoltowski, Martin Haardt, Cherian P. Mathews. *Closed-Form 2D Angle Estimation with Rectangular Arrays in Element Space or Beamspace via Unitary ESPRIT*, IEEE Transactions on Signal Processing, vol.44, No.2, February 1996.

[3] E.A Mohamed, Tan Zhan Zhong, *Adaptive Antenna Utilizing Power Inversion and Linear Constraint Minimum Variance Algorithms*, Chinese Journal of Aeronautics, vol.18, No.2, pp. 153-160, March 2005.

[4] Hank Rausch, *Jamming Commercial Satellite Communications During Wartime: An Empirical Study*, iwia, Fourth IEEE International Workshop on Information Assurance (IWIA'06), pp.109-118, 2006.

[5] Rec. ITU-R S.1524. Coordination identification between geostationary-satellite orbit fixed-satellite service networks, 2001.

[6] European Satellite Operator Association. Today's Situation & Ongoing Trends in the Fixed Satellite Situation (FSS) Global Market ESOA Picture. http://www.esoa.net/v2/docs/public_cband/ESOA_CBand_FSSTrends.pdf